

Biomechanical analysis of blast-induced traumatic brain injury

Mohammad Hossein Lashkari¹ MD, Ata Koohian² PhD, Kambiz Kangarlou^{*3} PhD

¹Department of Surgery, AJA University of Medical Sciences, Tehran, Iran.

²Department of Physics, University of Tehran, Tehran, Iran.

³Postdoctoral Researcher, Department of Biomedical Engineering, Amirkabir University of Technology, Tehran, Iran.

ABSTRACT

Purpose: Blast-induced traumatic brain injury (bTBI) is one of the causes of death or permanent invalidity which can occur unexpectedly in both military and civilian populations. This study set out to conduct a combined Eulerian-Lagrangian computational analysis of the interaction between a single planar blast wave and a human head in order to assess the extent of intracranial shock wave generation and its potential for causing traumatic brain injury.

Materials and Methods: To investigate the mechanical response of human brain to blast waves and to identify the injury mechanisms of TBI, a three-dimensional finite element model consisting of the scalp, skull, cerebrospinal fluid (CSF) and brain was developed from the imaging data of a human head. The mechanical properties of brain tissue were obtained from the literature.

Results: Throughout the loading regime, CSF acted as a protective layer for brain tissue by absorbing shear strain energy. Biomechanical loading of the brain was governed by direct wave transmission, structural deformations, and wave reflections from tissue-material interfaces.

Conclusion: The brain experiences a complex set of direct and indirect loadings emanating from different sources (reflections from tissue interfaces and skull deformation) at different points of time. The flow dynamics strongly depend on geometry (shape, curvature) and structure (flexural rigidity, thickness) of a specimen and should be considered in understanding biomechanical loading pattern.

Keywords: blast wave; traumatic brain injury; finite element analysis; viscoelastic material; Ansys.

AMHSR 2014;12:50-57
www.journals.ajajums.ac.ir

INTRODUCTION

Explosive devices used on a soldier in the battle field can cause severe and complicated injuries. Many factors can influence the severity and location of blunt trauma injuries a soldier receives from a blast event. The dispersal pattern and intensity of the blast wave is affected by the shape of weapon and the type of explosives used. The surrounding environment (air or water) can also change the dynamics of the blast. Also, reverberations and reflection of the blast wave can develop when the explosive device is used inside an enclosed structure. For example, explosive devices placed in tunnels can

focus the direction and intensity of a blast. The soldier's position and orientation in relation to the blast wave can also contribute to his physical impairment. Any of these factors can cause complicated injuries in soldiers such as blast lung, hemorrhaging, abdominal injuries, etc.

Traumatic brain injury (TBI) is a signature injury of the recent wars, affecting a majority of the military casualties. With the increased incidence of global terrorism against nonmilitary targets, new attention has been directed toward injuries in civilian populations. The employment of powerful improvised explosive devices (IEDs) by terrorists has also necessitated the

need to understand the nature of injuries caused by such devices.

It is speculated that blast-induced traumatic brain injury (bTBI) is a stress wave dominated phenomenon as opposed to a rotational acceleration/deceleration-induced injury, typically associated with the impact injuries commonly encountered in sports and automobile accidents.¹ The 15 point Glasgow coma scale² defines the severity of a TBI in mild (13-15), moderate (9-12), severe (3-8), and vegetative states (<3). As it is indicated in Table 1, the detection of injury is difficult or impossible using standard neuro-imaging techniques, especially for mild injury. Consequently, research on bTBI in humans certainly lacks clinically-based evidence, causing it to be confused with post-traumatic stress disorder which shows more or less identical symptoms.³

Our current understanding of the specific loading pathways and mechanisms of blast-induced neurotrauma remains incomplete. This is particularly detrimental to medical personnel and patients, since often times bTBI (especially in mild and moderate states) goes undetected with no available diagnosis through neuroradiology or neurophysiology. Psychological examination may or may not be able to reveal this ailment.⁴ Blast explosions can result in primary (pure blast), secondary (interaction with shrapnel or fragments), tertiary (impact with environmental structures), or/and quaternary (toxic gases) effects. This study has focused on the effect of primary blast which is likely in the range of mild TBI. It was expected that primary blast TBI be directly induced by pressure differentials across the skull, fluid, soft tissue interfaces and be further reinforced by the reflected stress waves within the cranial cavity, leading to stress concentrations in certain regions of the brain.

Thus, this study set out to characterize the effects of blast waves produced by various explosions on the resulting tissue level response of the brain using an anatomically inspired finite element model of human head combined with shock physics. The von Mises stress and pressure contours at different times and displacement history plots were also recorded.

MATERIALS AND METHODS

Blast wave parameters

Explosions are physical phenomena that result in the sudden release of energy; they may be chemical (typical rapid exothermic oxidation of a solid or liquid material into gaseous reaction products), nuclear or mechanical (for example pressure driven by rupture of a membrane or vessel). Typically, explosion reactions are completed within a few microseconds.⁵ Friedlander has described a typical pressure-time profile of an explosion in a free field, i.e. without reactions (Figure 1).⁶

The pressure-time history of a spherical blast can be expressed in the form of the Friedlander equation, based on the Sedov-Taylor blast wave solution:⁷

$$P(t) = P_0 + (P_{pos} - P_0) \left[1 - \frac{(t - t_a)}{t_{pos}} \right] e^{-b \frac{(t - t_a)}{t_{pos}}} \quad (1)$$

The parameter, b describes the decay of the curve, P_0 is the ambient air pressure and t_a is the time at peak positive over pressure. Recently, Teich and Gebekken⁸ have proposed a new formula to compute the wave decay parameter, which is $b = 1.5Z^{-0.38}$ ($01 < Z < 30$) and based on Larcher and colleagues⁹, $b = 5.2777Z^{-1.1975}$. The equations 2-10 were presented to compute peak positive

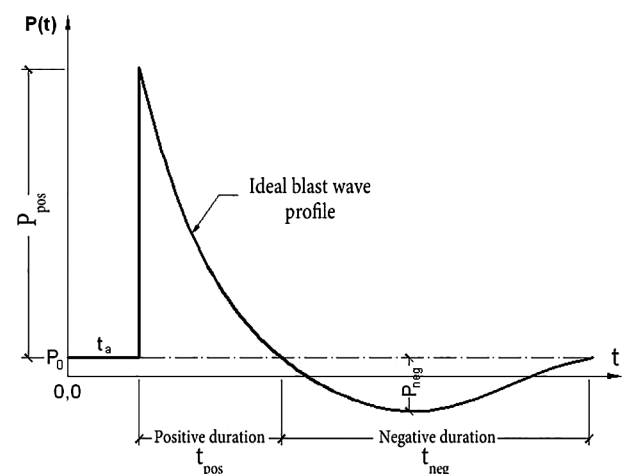


Figure 1. Ideal blast wave profile vs. time relation at a fixed point as defined by the biphasic Friedlander¹ equation.

Table 1. Classification of traumatic brain injury (TBI) severity.²

Criteria	Severity		
	Mild	Moderate	Severe
Loss of consciousness	0 – 30min	30min < t < 24hours	> 24hours
Alteration of mental state	Briefly < 24hours	> 24hours	> 24hours
Post-traumatic amnesia	0 – 1day	1day < t < 7days	> 7days
Glasgow coma scale score	13 – 15	9 – 12	< 9
Structural neuro-imaging	Normal	Normal/abnormal	Abnormal

over pressure (P_{pos}) variation with scaled distance (z), the positive phase of duration (t_{pos}) and the positive impulse (I_{pos}).

Based on the analysis of several experimental data, Henrych¹⁰ presented the following equations to compute peak over pressure, impulse and positive phase of duration:

$$P_{pos} = \begin{cases} \frac{14.072}{z} + \frac{5.540}{z^2} - \frac{0.357}{z^3} + \frac{0.00625}{z^4} \text{ (bar)} & (0.05 < z < 0.3) \\ \frac{6.194}{z} - \frac{0.326}{z^2} + \frac{2.132}{z^3} \text{ (bar)} & (0.3 < z < 1) \\ \frac{0.662}{z} + \frac{4.05}{z^2} + \frac{3.228}{z^3} \text{ (bar)} & (1 < z < 10) \end{cases} \quad (2)$$

$$t_{pos} = e^{(-2.75 + 0.27 \log z) + \log W^{1/3}} \text{ (mS)} \quad (3)$$

In addition, Kinney and Grahm¹¹ presented the following equations to compute peak over pressure, impulse and positive phase of duration:

$$P_{pos} = P_0 \frac{808 \left[1 + \left(\frac{z}{4.5} \right)^2 \right]}{\sqrt{\left[1 + \left(\frac{z}{0.048} \right)^2 \right]} \times \sqrt{\left[1 + \left(\frac{z}{0.32} \right)^2 \right]} \times \sqrt{\left[1 + \left(\frac{z}{1.35} \right)^2 \right]}} \text{ (bar)} \quad (4)$$

$$t_{pos} = W^{1/3} \frac{980 \left[1 + \left(\frac{z}{0.54} \right)^{10} \right]}{\left[1 + \left(\frac{z}{0.02} \right)^3 \right] \times \left[1 + \left(\frac{z}{0.74} \right)^6 \right] \times \sqrt{\left[1 + \left(\frac{z}{6.9} \right)^2 \right]}} \text{ (millisecond)} \quad (5)$$

$$I_{pos} = \frac{0.067 \sqrt{1 + \left(\frac{z}{0.23} \right)^4}}{Z^2 \sqrt{1 + \left(\frac{z}{1.55} \right)^3}} \text{ (bar - ms)} \quad (6)$$

And Sadovskiy¹² presented the following equations for peak over pressure, impulse and positive phase of duration based on explosion data analysis:

$$P_{pos} = 0.085 \frac{W^{1/3}}{R} + 0.3 \left(\frac{W^{1/3}}{R} \right)^2 + 0.8 \left(\frac{W^{1/3}}{R} \right)^3 \text{ (MPa)} \quad (7)$$

$$t_{pos} = 1.2 \sqrt[6]{W} \sqrt{R} \text{ (ms)} \quad (8)$$

$$I_{pos} = 200 \frac{W^{2/3}}{R} \text{ (Pa - s)} \quad (9)$$

Where W is the charge weight in kg, Z is the scaled distance in m and expressed as:

$$Z = \frac{R}{W^{1/3}} \text{ (m/kg}^{1/3}\text{)}, \quad R_2 = R_1 \left(\frac{W_2}{W_1} \right)^{1/3} \quad (10)$$

Finite element models of the explosive, air material and the head

Finite element analysis was performed using Ansys 3D. The complete definition of a transient non-linear dynamics problem (such as the interactions of blast waves with the human head) entails the knowledge of the material models that define the relationships between the variables pressure, mass-density, energy-density, temperature, etc. These relations typically involve an equation of state, a strength model and a failure model for each constituent material.

Modeling of the explosive. The detonation and expansion of the TNT explosive materials was described using the Jones-Wilkins-Lee (JWL) equation of state along with a high explosive material definition. The JWL equation is described as:

$$p_{EOS} = A \left(1 - \frac{\omega}{R_1 V} \right) e^{-R_1 V} + B \left(1 - \frac{\omega}{R_2 V} \right) e^{-R_2 V} + \omega \frac{E_0}{V} \quad (11)$$

Where $V = \rho_0$ (initial density of an explosive) / ρ (density of detonation gas). E_0 is specific internal energy per unit mass. A , B , R_1 , R_2 , ω are JWL fitting parameters. The parameters for the JWL equation can be found, for example, in Dobratz and Crawford.¹³ The values used for TNT explosives are shown in Table 2.

Air material model. The Eulerian domain was filled with air. Air was modeled as an ideal gas and, consequently, its equation of state was defined by the ideal-gas gamma-law relation as:

$$P = (\gamma - 1) \frac{\rho}{\rho_0} E \quad (12)$$

Where P is the pressure, γ the constant-pressure to constant-volume specific heats ratio (1.4 for a diatomic gas like air), ρ_0 (1.225 kg/m³) the initial air mass density, and ρ the current density. For equation (12) to yield the standard atmosphere pressure of 101.3 kPa, the internal volumetric energy density E was set at 253.4 kJ/m³, which corresponds to the air mass specific heat of 717.6 J/kg-K and a reference temperature of 290 K.

Brain-tissue materials model. Various numbers of head components have been modeled by different authors. The head was modeled with Lagrangian elements and directly from the design CAD 3D drawings (Figure 2).

Table 2. Jones-Wilkins-Lee (JWL) and material parameters for TNT explosive.¹³

ρ_0 (kg/mm ³)	V (m/s)	A	B	R_1	R_2	ω	E_0 (GPa)
0.63e-6	6930	374	3.21	4.15	0.95	0.3	7

Keys: ρ_0 , initial density of an explosive; V , Detonation velocity; E_0 , specific internal energy per unit mass; A , B , R_1 , R_2 , ω are Material constant (GPa).

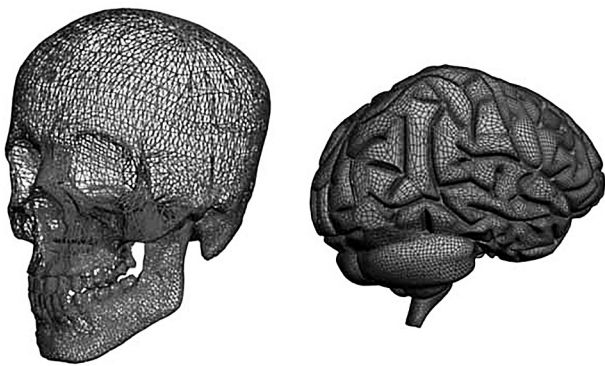


Figure 2. Finite element model of the human head.

The image data were segmented into three different tissue types of the head: (1) skull, (2) cerebrospinal fluid (CSF) and (3) brain. The brain is surrounded by 140 ml of CSF. This fluid cushions the brain from mechanical shock and, during normal movement, shrinking and expansion of the brain is quickly balanced by an increase or decrease of CSF that can flow from the cranial cavity into the spinal cavity through the foramen magnum. The skull and CSF are modeled as linear, elastic, isotropic materials with properties adopted from the literature.¹⁴ Hrapko and colleagues¹⁵ have presented an overview of available literature on the material properties of the brain tissue. Brain tissue can generally be defined as a heterogeneous, viscoelastic solid, consisting up to 80% of the water. The material is almost incompressible (Poisson's ratio $\nu \sim 0.5$), and can be assumed to only deform in shear.¹⁶ So the brain was modeled with an elastic volumetric response and viscoelastic shear response.

In this study, a material model was used which assumes linear viscoelastic and isotropic behavior for both grey and white matter. The standard linear solid model was applied to characterize the shear behavior, and the shear relaxation modulus was described by:

$$G(t) = G_{\infty} + (G_0 - G_{\infty})e^{-\beta t} \quad (13)$$

in which G_0 is the short-term shear modulus, G_{∞} is the long-term shear modulus, and β is a decay constant. The material parameters used were the same as those in Zhang and colleagues¹⁷ (Table 3). The interface between all these tissue types was modeled as a tied contact. The

bottom of the neck was constrained in all six degrees of freedom to avoid rigid body motion.

RESULTS

Mechanics of blast wave and head interactions

When the blast wave impacts the head, it gives rise to various types of waves which are defined as:

- Surface pressure wave: surface pressure wave is a reflected shock wave on the surface of the head. Surface pressure wave indicates where the shock front is at a given time. In this work, loading induced by the surface pressure wave was considered as a “direct load” since the surface pressure wave transmits energy directly into the brain.¹⁸
- Structural wave in the skull: when the blast wave impacts the head, it gives rise to a stress wave traveling through the skin, skull and brain. Because of its acoustic properties, stress wave in the skull travels much faster than in the other soft tissues of the head. Therefore, the stress wave traveling through the skull was monitored in this work and it was defined as a structural wave in the skull. The loading induced by structural wave was considered an “indirect load” since the load is because of structural dynamical deformation.¹⁸

Relation between surface pressure, cranial and intracranial stress

One of the reasons for developing a finite element head model is to investigate blast head injury. The value of von Mises stress has been used to examine the brain injury risk.¹⁹ Figure 3 shows the associated distribution of the von Mises equivalent stress and surface pressures over skull at $t = 0.5$ and 1.0 ms after explosion of 0.5 kg TNT-equivalent explosive charge at a distance of 0.80 m. Incident peak overpressure corresponding at forehead was 0.23 MPa and the peak surface pressure was 0.553 MPa. Thus, the pressure amplification (the ratio of reflected pressure to incident pressure) was 2.40 due to fluid–structure interaction effects. Figure 4 shows the surface pressures, pressure in the skull, and pressure in the brain at sections 1, 2, 3 and 4 of the human head model. Various locations at which the pressure history was plotted have been marked. The peak surface pressure gradually decreased from locations 1 to 4 as the shock

Table 3. Viscoelastic material properties of the brain.¹⁴

Tissue	ρ (kg/m ³)	K (Pa)	G_0 (Pa)	G_{∞} (Pa)	β (s ⁻¹)
Grey matter	1040	2.19E+9	3.4E+4	6.4E+3	400
White matter	1040	2.19E+9	4.1E+4	7.8E+3	400

Keys: ρ , density; K , bulk modulus; G_0 , short-term shear modulus; G_{∞} , long-term shear modulus; β , decay constant.

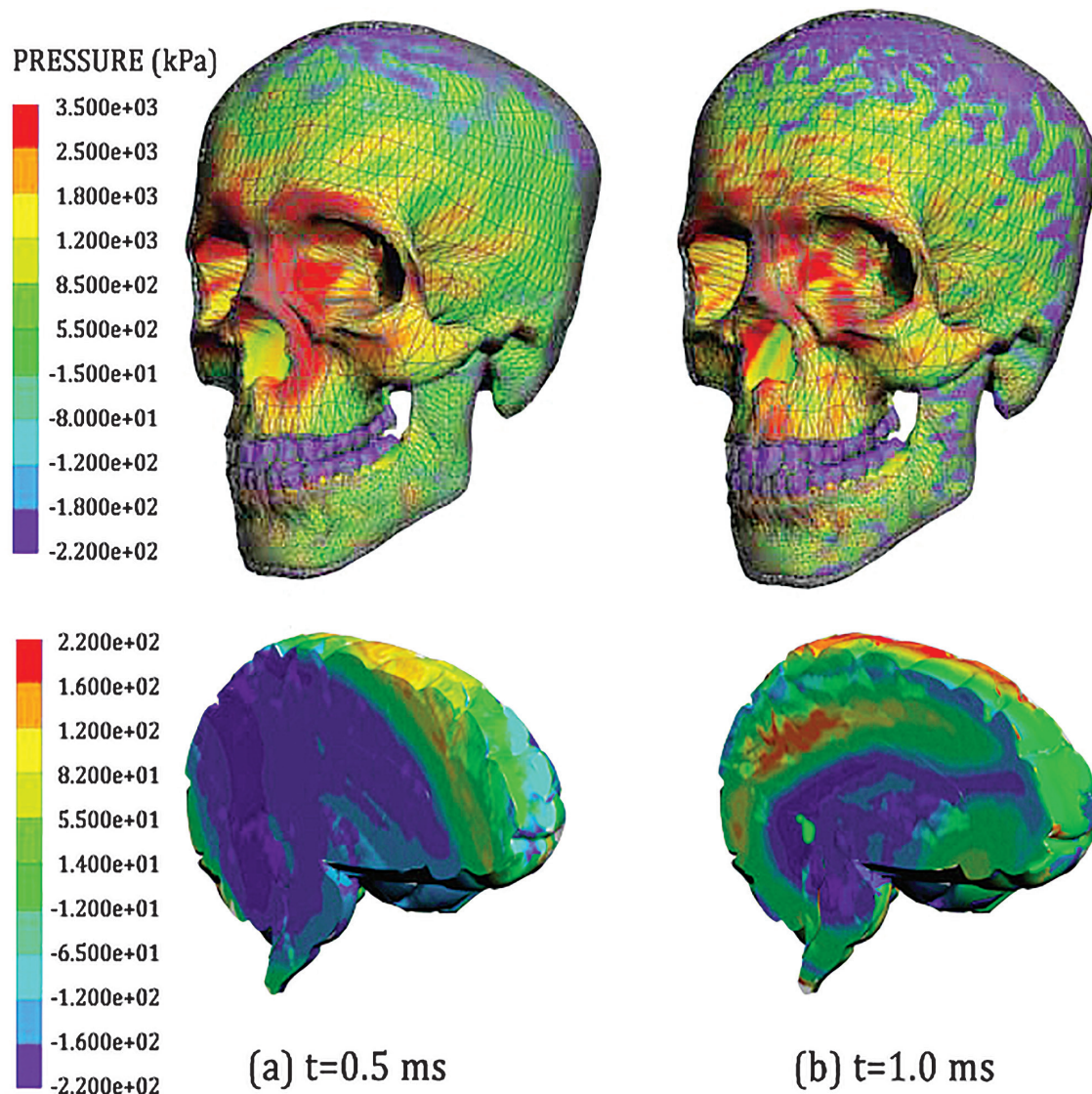


Figure 3. The associated distribution of the pressures over skull and brain, (a) at $t=0.5$ ms, (b) at $t=1.0$ ms after explosion. The pressure limits are -0.28 and 3.51 MPa.

wave traversed the head.

Strain magnitude was largely dependent on the impulse of the blast, and primarily caused by the radial coupling between the brain and deforming skull. The largest predicted strains were generally less than 10%, and occurred after the shock wave passed through the head. For blasts with high impulses, CSF cavitations had a large role in increasing strain levels in the cerebral cortex and per ventricular tissues by decoupling the brain from the skull.

DISCUSSION

The intracranial pressure, shear stresses and strains were suggested as injury predictors for TBI. In 1980, Ward and colleagues²⁰ proposed a peak intracranial pressure

concussion threshold of 235 kPa through animal studies and minor or no brain injury for intracranial pressure below 173 kPa. In 1999, Anderson and colleagues²¹ reported through caprine tests and numerical analysis that shear stresses over the range of 8–16 kPa could cause widespread axonal injuries. In addition, Kang and colleagues suggested through computational simulation of motorcyclist accidents, that shear stresses over the range of 11–16.5 kPa could lead to significant brain injury. Morrison and colleagues²² showed that maximum principal strain can be used as a measure of central nervous system injuries such as diffuse axonal injury and cell death. Bain and Meaney²³ also demonstrated that diffuse axonal injury is practically a function of distortion (strain), rather than pressure, which maybe

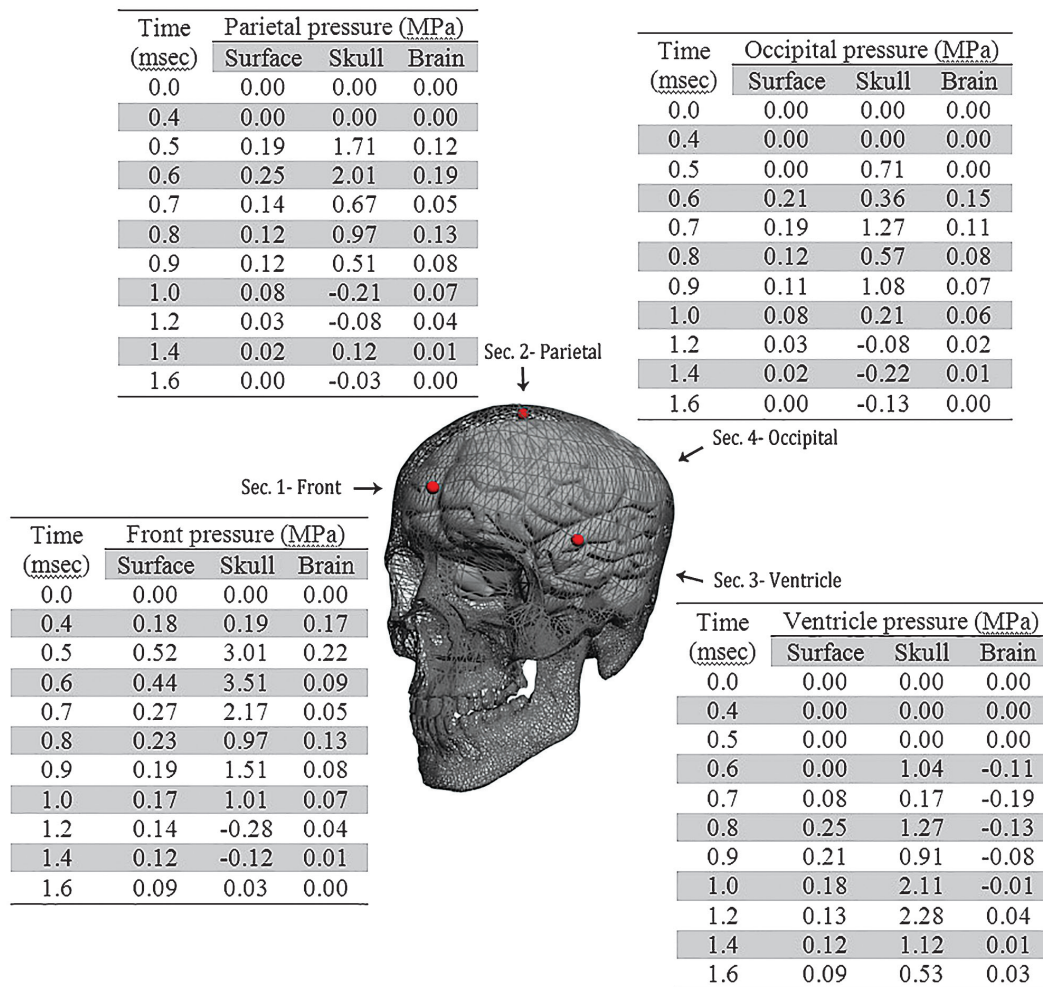


Figure 4. Relationship between surface pressure, cranial and intracranial stress.

a more relevant parameter to predict head injury. They estimated a principal strain threshold for axonal damage of 21% for morphological axonal injury, and 18% for deterioration of nerve function, all based on experiments done on optic nerves of adult guinea pigs.²⁴

TBI resulting from sports-related injuries has a longer history of study than bTBI. Zhang and colleagues²⁵ conduct numerical experiments using a finite element model to recreate helmet to helmet collisions in football, in order to determine the best indicators of injury based on comparison to actual outcomes. They concluded that shear stress in the midbrain of the brainstem was the best predictor based on their sampling ($n = 24$), and estimated that shear stresses of 6.0, 7.8, and 10.0 kPa in the midbrain correlated to 25%, 50%, and 80% probability of mild TBI diagnosis, respectively. In this study, serious brain injury was correlated to peak intracranial pressures greater than 235 kPa, while peak pressures below 173 kPa resulted in

minor or no injury. Predicted shear strain was highest at the interface between the brain and the CSF.

We have conducted a modeling and simulation investigation of the wave motion that occurs within the human brain as a result of blast loading to the head. The results predicted significant levels of pressure and deviatoric stress occurring at focal regions in the brain within the first 2 ms of the blast event. As the blast wave encounters the head, it directly transmits some energy to the brain and at the same time initiates structural wave in the skull. The frontal portion of the brain had the highest pressures corresponding to the location of initial impact, and peak pressure attenuated by 40–60% as the wave propagated from the frontal to the occipital lobe. Predicted brain pressures were primarily dependent on the peak overpressure of the impinging blast wave, and the highest predicted brain pressures were 30% less than the reflected pressure at the surface of blast impact.

Figure 4 shows the sequence of the blast wave passing through the skull and brain of a human head. Once the blast wave front reaches the skull, it is subject to a high resistance, which in turn leads to partial reflection of the blast wave from the skull. The other part of the wave compresses the skull wall, sending a pressure wave into the CSF. This pressure wave will propagate in all three dimensions inside the skull. The wave in the direction normal to the skull thickness squeezes the CSF fluid inside, causing the local increase of the pressure inside the CSF fluid. This high pressure in turn pushes the brain downward. The sequence clearly shows the transport of wave from blast into the brain stress. The decompression on CSF leads to a local lower pressure zone, which sucks the brain into it and may cause potential damage in this region due to high stress. This pressure wave in the CSF is much faster than that of the pressure wave in the air outside of the skull, since the speed of sound in the skull, brain and CSF is about 4–8 times faster than that in the air.²⁶

CONCLUSION

From an engineering point of view, the final objective of brain injury research is to provide a predictive tool such as a finite element model that can aid in injury diagnosis and design of protective devices. A well validated finite element model can be such a powerful tool, especially when brain injury experiments are difficult and expensive to carry out.

Our results clarify that the flow dynamics strongly depend on geometry (shape, curvature) and structure (flexural rigidity, thickness) of a specimen and should be considered in understanding biomechanical loading pattern. Any given point, the brain experiences a complex set of direct and indirect loadings emanating from different sources (reflections from tissue interfaces, skull deformation) at different points of time.

An important objective of this research is to create a foundation for continued research and continue refinement of finite volume models. Specific areas for future work can include: (a) a more realistic boundary condition at the head-neck junction and interface condition between the skull and the brain; (b) modeling of membranes and other substructures based on better imaging and processing techniques; and (c) increasing the accuracy of material properties. More realistic behavior can be achieved through better representation of the physical material properties as well as their geometries. Non-linear representation of visco-elasticity may be critical in accurately modeling the response of the brain.

CONFLICT OF INTEREST

None Declared.

REFERENCES

1. Nyein MK. *Computational modeling of blast-induced traumatic brain injury* [thesis]. Cambridge, USA: Massachusetts Institute of Technology;2010.
2. Green SM. Cheerio, laddie! Bidding farewell to the Glasgow coma scale. *AnnEmergMed*.2011;58:427-30.
3. Eldar GA, Dorr NA, De Gasperi R, et al. Blast exposure induces post-traumatic stress disorder-related traits in a rat model of mild traumatic brain injury. *J Neurotrauma*. 2012;29:2564-75.
4. Sundaramurthy A, Alai A, Ganpule S, et al. Blast-induced biomechanical loading of the rat: experimental and anatomically accurate computational blast injury model. *J Neurotrauma*. 2012;29:2354-64.
5. Goel MD, Matsagar VA, Gupta AK, et al. An abridged review of blast wave parameters. *DefenceSci J*. 2012;62:300-6.
6. Chafi MS, Karami G, Ziejewski M. Numerical analysis of blast-induced wave propagation using FSI and ALE multi-material formulations. *Int J Impact Engin*. 2009;36:1269-75.
7. Sedov LI. Propagation of strong shock waves. *J App Math Mech*. 1946;10:241-50.
8. Teich M, Gebbeken N. The influence of the under pressure phase on the dynamic response of structures subjected to blast loads. *Int J Prot Str*. 2010;1:219-34.
9. Larcher M, Herrmann N, Stempniewski L. Explosions simulation leichter Hallenhüllkonstruktionen. *Bauingenieur*. 2006;81:271-7.
10. Henrych J. *The dynamics of explosion and its use*. Amsterdam: Saunders Elsevier;1979.
11. Kinney GF, Graham KJ. *Explosive shocks in air*. Berlin: Springer;1985.
12. Sadovskiy MA. Mechanical effects of air shockwaves from explosions according to experiments. In: Sadovskiy MA. *Selected works: Geophysics and physics of explosion*. Moscow: Nauka Press;2004.
13. Dobratz BM, Crawford PC. *LLNL Explosives Handbook: Properties of Chemical Explosives and Explosive Simulants*. Livermore: Lawrence Livermore National Laboratory; 1985.
14. Chen Y, Ostoj-Starzewski M. MRI-based finite element modeling of head trauma: Spherically focusing shear waves. *Acta Mech*. 2010;213:155-67.
15. Hrapko M, van Dommelen JAW, Peters GWM, et al. On the consequences of non linear constitutive modeling of brain tissue for injury prediction with numerical head models. *Int J Crashworthiness*. 2009;14:245-57.
16. Newman JA, Shewchenko N, Welbourne E. A proposed new biomechanical head injury assessment function - the maximum power index. *Stapp Car Crash J*. 2000;44:215-47.
17. Zhang L, Yang KH, King AI. A proposed injury threshold for mild traumatic brain injury. *J Biomech Eng*. 2004;126:226-36.

18. Ganpule S, Alai A, Plougonven E, et al. Mechanics of blast loading on the head models in the study of traumatic brain injury using experimental and computational approaches. *Biomech Model Mechan*. 2013;12:511-33.
19. Marjoux D, Baumgartner D, Deck C, et al. Head injury prediction capability of HIC, HIP, SIMon and ULP criteria. *Accid Anal Prev*. 2008;40:1135-48.
20. Ward CC, Chan M, Nahum AM. *Intracranial pressure – A brain injury criterion*. Paper presented at: Proceedings of the 24th Stapp Car Crash Conference, SAE Paper No. 801304; October 15-17, 1980; Troy, Michigan.
21. Anderson RWG, Brown CJ, Blumbergs PC, et al. *Mechanisms of axonal injury: An experimental and numerical study of a sheep model of head impact*. Paper presented at: Proceedings of International Conference on the Biomechanics of Impact; September 23-24, 1999; Sitges, Spain.
22. Morrison B, Cater HL, Wang CC, et al. A tissue level tolerance criterion for living brain developed with an in vitromodel of traumatic mechanical loading. *Stapp Car Crash J*. 2003;47:93-105.
23. Meaney DF, Smith DH, Shreiber DI, et al. Biomechanical analysis of experimental diffuse axonal injury. *J Neurotrauma*. 1995;12:689-94.
24. Chafi MS, Ganpule SG, Gu L, et al. Dynamic response of brain subjected to blast loadings: influence of frequency ranges. *Int J Appl Mech*. 2011;3:803-23.
25. Zhang L, Yang KH, King AI. Comparison of brain responses between frontal and lateral impacts by finite element modeling. *J Neurotrauma*. 2001;18:21-30.
26. Imielinska C, Przekwas A, Tan XG. Multi-scale visual analysis of trauma injury. *Information Visualization*. 2006;5:279-89.

Corresponding Author:

Kambiz Kangarlou, PhD

Address: No 2, 6th St., Iranzamin St., Shahrak Gharb District, Tehran, Iran.

Postal Code: 1465693493

Tell: +98 21 88363337

Fax: +98 21 88363337

Cell Phone: +98 9122132379

E-mail: kangarloo_kambiz@yahoo.com

Received August 2013

Accepted January 2014